A THEORETICAL RADIAL LOAD DISTRIBUTION IN SCREW THREADS

By

RICHARD MILLARD GILMORE II

Bachelor of Science

Oklahoma Agricultural and Mechanical College

Stillwater, Oklahoma

1952

Submitted to the faculty of the Graduate School of
the Oklahoma Agricultural and Mechanical College
in partial fulfillment of the requirements
for the degree of
MASTER OF SCIENCE
May, 1953

OKLAHOMA STATE UNIVERSITY

A THEORETICAL RADIAL LOAD DISTRIBUTION

IN SCREW THREADS

Thesis Approved:

Ladislaus J. Fila
Thesis Adviser

B. M. Aldrich
Major Adviser

O. C. McDaniel
Dean of the Graduate School

PREFACE

Screw thread fasteners are used extensively to join component parts of machines, and in size, shape, and strength screw threads have been standardized to a high degree. However, in the design of screw threads, theory lags far behind practice; as yet, no adequate theory has been developed which will give stress values throughout the thread in agreement with experimental test results.

The purpose of this paper is to obtain a theoretical radial load distribution on the screw thread by assuming a segment of the thread to be a cantilever beam. Since the beam is short and deep, it is necessary to consider the effects of both shear and bending moment upon the deflection curve of the loaded beam. The theoretical load distribution is obtained by the use of statics, physical properties of the material, and assumptions as to the geometry of the deflected beam.

My thanks are due to Professor L. J. Fila for his guidance and assistance to me in the preparation of this thesis and in many matters pertaining to my work. I also appreciate the constructive criticisms and suggestions made by Professor C. M. Leonard, and I wish to acknowledge the assistance of my wife, Albiette Gilmore, in typing and proofreading the manuscript.

TABLE OF CONTENTS

LIST OF TABLES

LIST OF ILLUSTRATIONS

LIST OF SYMBOLS

A	area, square inches
a	load distribution coefficient
B	width of tooth segment, inches
C	constant
c	distance, inches
D	constant
d	distance, inches
E	Modulus of elasticity, pounds per square inch
F	total external load on tooth segment, pounds
f	flexure (subscript)
G	shear modulus, pounds per square inch
H	constant
I	moment of inertia of area
J	constant
K	rigidity constant
k	stress factor for a rectangular cross section
ℓ	length, inches
M	constant; moment, inch pounds
m	mean (subscript)
N	constant
n	constant; number
P	pitch of threads, inches
p	distance, inches

S	shear load, pounds
s	stress, pounds per square inch; shear (subscript)
t	thread depth, inches
W	work, inch pounds
w	load distribution, pounds per inch
x	location of a section
y	deflection, inches
θ	location of a section, $(x - \frac{t}{2})$
ϕ	a constant, $(t/2)$
μ	Poisson's ratio

CHAPTER I

INTRODUCTION

This thesis is a continuation of work done on a theory of stress distribution in screw threads initiated in 1951 by Raymond E. Chapel.[1] In his work Mr. Chapel substituted for the screw threads a continuous elastic layer having a thickness equal to the thread depth. Mr. Chapel made the following two assumptions: (1) the layer had a perfect bond at the minor diameter of the bolt and the major diameter of the nut, and (2) the layer possessed the same rigidity as the threads. A physical comparison of the assumed elastic-layer joint with the actual nut and bolt is shown in Figure 1.

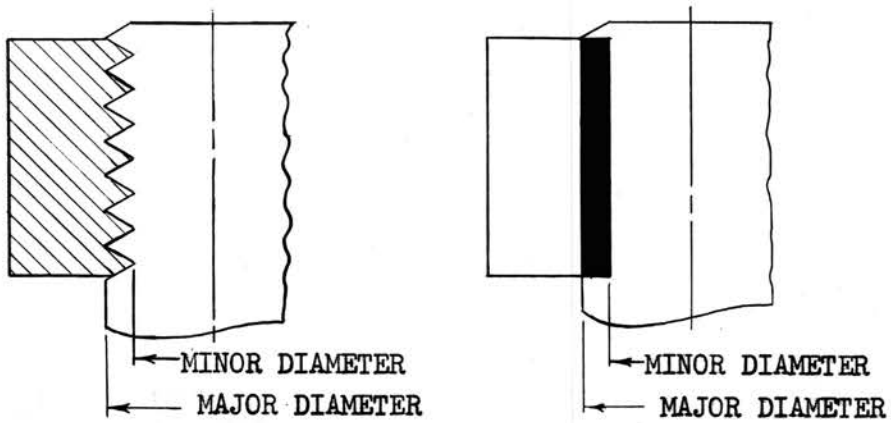

Fig. 1.—Cross-sectional views of the actual threaded joint and the hypothetical elastic-layer joint. (Courtesy of Raymond E. Chapel).[2]

---

[1]Raymond E. Chapel, "A Contribution to the Theory of Load Distribution in Screw Threads" (unpublished M. S. thesis, Department of Mechanical Engineering, Oklahoma A. & M. College, 1951).

[2]Ibid., p. 5.

By the elastic-layer theory, an axial tensile load on the bolt was assumed to be distributed through the layer, becoming a compressive load in the nut. The axial stress was found to vary from a value of zero at the end of the layer most remote from the tensile load in the bolt to a maximum value at the bottom of the nut. This type of stress distribution agrees fairly well with experimental photoelastic stress values as reported by M. Hetényi.[3]

In 1952, Gertrude H. Fila refined the theory further by applying the method of least work to a solution of the stresses in screw threads.[4] Axial stress distribution in the elastic layer was shown to be in the form of one half of a catenary, the minimum stress being at the end of the thread with the maximum being at the bottom of the nut. This type of stress distribution gave even better agreement with experimental data than was obtained by Mr. Chapel.[5]

To determine the value of a rigidity constant needed in the method of least work, Mrs. Fila assumed the screw thread tooth to be a cantilever beam carrying a concentrated load at the free end. The load used was the shear force at the thread root; i. e., the shear stress in the elastic layer at the point multiplied by the area of the thread segment root.[6]

The aim of this thesis is to determine the radial load distribution along the thread segment by considering the deflection of the

---

[3]M. Hetényi, "A Photoelastic Study of Bolt and Nut Fastenings," A.S.M.E. Transactions, 65 (1950), pp. A-93 through A-100.

[4]Gertrude H. Fila, "Load Distribution in Screw Threads by the Method of Least Work" (unpublished M. S. thesis, Department of Mechanical Engineering, Oklahoma A. & M. College, 1952).

[5]Ibid., p. 20.

[6]Ibid., p. 25.

thread due to flexure and shear. Although the elastic-layer theory does not depend upon the radial distribution of load on the tooth segment for its derivation or validity, a knowledge of the configuration of the load imposed upon the thread could be helpful in the evaluation of the rigidity of the threaded joint (analogous to the elasticity of the elastic layer), in the design of threads for specific purposes, and in the understanding of the limitations of present thread fasteners.

CHAPTER II

DEVELOPMENT OF THE THEORY

Basic Assumptions

While the elastic-layer theory is applicable for the evaluation of axial stress distribution in a threaded member, in order to determine the radial load distribution, it becomes necessary to use characteristics of the actual threaded joint, which, because of the geometry and properties of the actual thread, do not lend themselves to simple analysis. For example, some of the variables encountered are: (1) the thread is helical in form with the helix angle varying with different forms and sizes of thread, (2) the thread angle (that is, the angle included between the sides of the thread measured in the axial plane) also varies with the thread form, (3) the mating nut and bolt are often of different materials, and (4) the class of fit, or amount of clearance existing between the mating threads, depends upon the method of manufacture and purpose for which the thread is intended. In view of these variables, some simplifying assumptions are necessary.

A first simplification will be to assume each thread segment to act as a cantilever beam of uniformly varying cross section. The load upon the beam will be imposed by an adjacent tooth segment of the mating thread.

A second simplification will be to consider a single form of thread to be representative of most V-type threads. The form used

will be the modification by Mrs. Fila[1] of the Whitworth 55° thread.[2] Its principal characteristics are given in Figure 2.

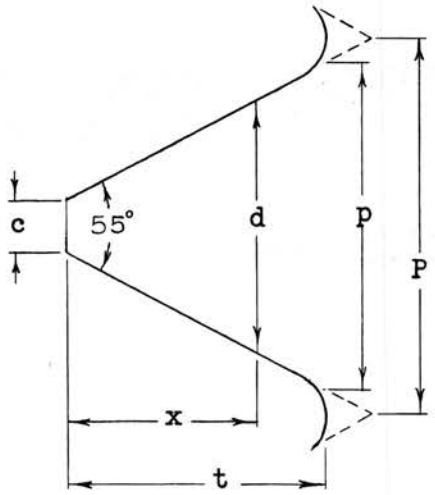

Fig. 2.—Beam Characteristics of Screw Threads (Adapted from Gertrude H. Fila's Master's Thesis)[3]

The cross-sectional area of the beam at a distance x from the free end is

$$A = Bd = B\left[c + \frac{x}{t}(p - t)\right] = B\left(\frac{p - c}{t}\right)\left[\left(\frac{ct}{p - c}\right) + x\right] = D(J + x).$$

The moment of inertia of the section at x becomes

$$I = \frac{Bd^3}{12} = \frac{B}{12}\left[c + \frac{x}{t}(p - c)\right]^3 = \frac{B}{12}\left(\frac{p - c}{t}\right)^3\left[\frac{ct}{p - c} + x\right]^3$$

$$= C(J + x)^3.$$

Other assumptions are that the threads mate perfectly, and that

---

[1]Gertrude H. Fila, "Load Distribution in Screw Threads by the Method of Least Work" (unpublished M. S. thesis, Department of Mechanical Engineering, Oklahoma A. & M. College, 1952).

[2]Erik Oberg and F. D. Jones, Machinery's Handbook (New York, 1941), p. 1274.

[3]Fila, op. cit., p. 25.

both the nut and bolt are made of the same homogeneous material, thereby having identical physical properties.

Throughout this work, the sign convention which will be observed is shown below.

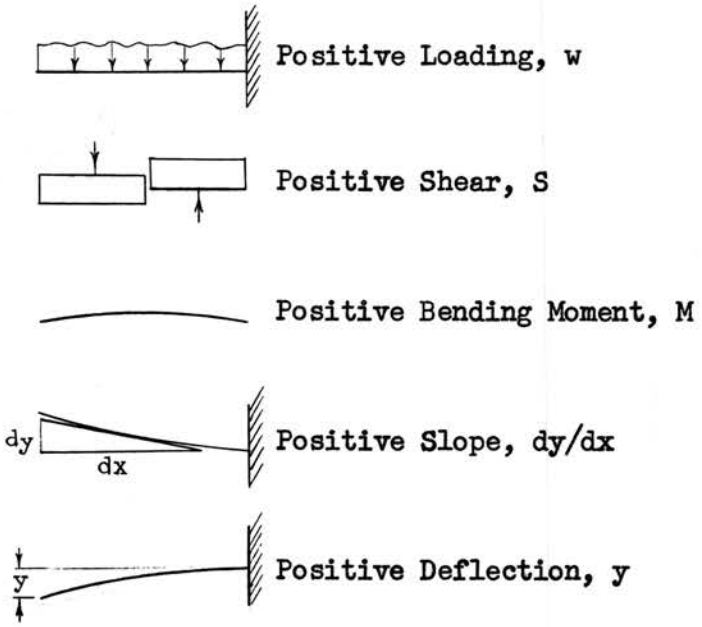

Development of the Curvature Equation

The effects of a local load applied at any point in the threaded joint may be observed by considering the center lines of two adjacent mating thread segments as shown in Figure 3.

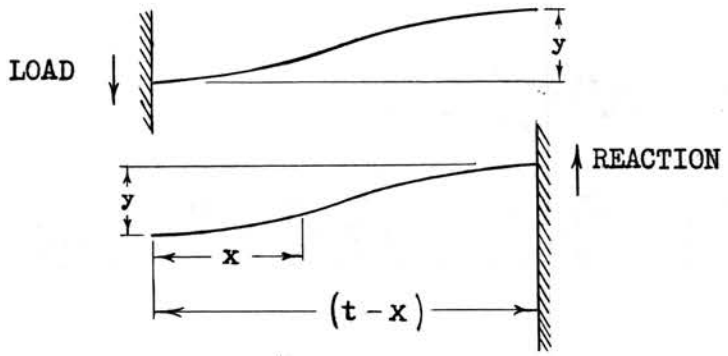

Fig. 3.—Center Line Displacement of Adjacent Threads Under Load

Since the mating threads are identical in size and composition, a load applied at the root of one thread (bolt) is resisted by a reaction force in the opposite direction at the root of the mating thread (nut). Thus, the deflection of the thread at x in the bolt would be identical to the deflection of the nut thread at (t - x), or the deflection curve for each thread must be anti-symmetric with respect to the point $x = \frac{t}{2}$.

In order to have an anti-symmetric deflection curve, it is apparent that the slope at x must be equal to the slope at (t - x); likewise, the curvature at x must be the negative curvature of (t - x). In this way it is seen that there are three necessary conditions which must be satisfied if the deflection curve be anti-symmetric.

$$y_x + y_{t-x} = y_{x=o} = \text{constant} \tag{1}$$

$$\left(\frac{dy}{dx}\right)_x - \left(\frac{dy}{dx}\right)_{t-x} = 0, \text{ and} \tag{2}$$

$$\left(\frac{d^2y}{dx^2}\right)_x + \left(\frac{d^2y}{dx^2}\right)_{t-x} = 0. \tag{3}$$

If the load distribution at x is $w = w(x)$, then the curvature due to flexure is

$$\left(\frac{d^2y}{dx^2}\right)_f = \frac{M}{EI} = \frac{\int_o^x \int_o^x w\, dx^2}{EI} \tag{4}$$

where E is the modulus of elasticity, and I is the moment of inertia of the section under consideration.

For a short deep beam such as the one under consideration the

deflection due to shear may be a large part of the total deflection. Therefore, the shear effects must be taken into account. Timoshenko and MacCullough[4] give the slope of the deflection curve due to shear as

$$\left(\frac{dy}{dx}\right)_s = -\frac{kS}{AG} = -\frac{k\int_o^x w\,dx}{AG} \tag{5}$$

where S/A is the average shear stress,

G is the modulus in shear, and

k is a numerical factor by which the average stress must be multiplied in order to obtain the shearing stress at the centroid of the cross section. For a rectangular cross section, k = 3/2.

Since it can be seen that the area of the cross section varies with x, Eq. (5) can be differentiated to obtain the curvature due to shear

$$\left(\frac{d^2y}{dx^2}\right)_s = -\frac{kw}{AG} + \frac{k\int_o^x w\,dx}{A^2G}\left(\frac{dA}{dx}\right). \tag{6}$$

The total curvature due to flexure and shear will be the sum of Eqs. (4) and (6),

$$\left(\frac{d^2y}{dx^2}\right) = \frac{\int_o^x\int_o^x w\,dx^2}{EI} - \frac{kw}{AG} + \frac{k\int_o^x w\,dx}{A^2G}\left(\frac{dA}{dx}\right). \tag{7}$$

The Load Distribution as a Power Series

The mating beams having identical deflection curves must have the same loading curve. The only way in which two threads in contact can

---

[4]S. Timoshenko and G. H. MacCullough, Elements of Strength of Materials (New York, 1935), p. 169.

have the same loading curve is for the curve to be symmetric about the midpoint, or $w_{(x)} = w_{(t - x)}$.

Symmetry may be satisfied by defining w as an even-powered series, such as

$$w_x = a_o + \frac{a_1}{t^2}(x - \frac{t}{2})^2 + \frac{a_2}{t^4}(x - \frac{t}{2})^4 + \ldots + \frac{a_n}{t^{2n}}(x - \frac{t}{2})^{2n}, \qquad (8)$$

and

$$w_{(t - x)} = a_o + \frac{a_1}{t^2}(t - x - \frac{t}{2})^2 + \frac{a_2}{t^4}(t - x - \frac{t}{2})^4 + \ldots$$

$$= a_o + \frac{a_1}{t^2}(\frac{t}{2} - x)^2 + \frac{a_2}{t^4}(\frac{t}{2} - x)^4 + \ldots = w_x.$$

The total shear will be the integral of the loading curve over the entire beam:

$$S_t = \int_o^t w\,dx = \left[a_o x + \frac{a_1}{3t^2}(x - \frac{t}{2})^3 + \frac{a_2}{5t^4}(x - \frac{t}{2})^5 + \ldots\right]_0^t$$

$$= a_o t + \frac{a_1}{3t^2}(\frac{t}{2})^3 + \frac{a_2}{5t^4}(\frac{t}{2})^5 + \ldots + \frac{a_1}{3t^2}(\frac{t}{2})^3 + \frac{a_2}{5t^4}(\frac{t}{2})^5 + \ldots$$

$$= a_o t + \frac{a_1}{t^2}(\frac{2}{3})(\frac{t}{2})^3 + \frac{a_2}{t^4}(\frac{2}{5})(\frac{t}{2})^5 + \ldots + \frac{a_n t}{(2n + 1)(2^{2n})}$$

$$= F, \text{ a constant.} \qquad (9)$$

The shear at point x is

$$S_x = \int_o^x w\,dx = a_o x + \frac{a_1}{3t^2}\left[(x - \frac{t}{2})^3 + (\frac{t}{2})^3\right] + \frac{a_2}{5t^4}\left[(x - \frac{t}{2})^5 + (\frac{t}{2})^5\right]$$

$$+ \ldots + \frac{a_n}{(2n+1)t^{2n}}\left[(x - \tfrac{t}{2})^{2n+1} + (\tfrac{t}{2})^{2n+1}\right], \qquad (10)$$

and the shear at point $(t - x)$ is

$$S_{(t-x)} = \int_o^{(t-x)} w\,dx = a_o(t-x) + \frac{a_1}{3t^2}\left[-(x - \tfrac{t}{2})^3 + (\tfrac{t}{2})^3\right]$$

$$+ \frac{a_2}{5t^4}\left[-(x - \tfrac{t}{2})^5 + (\tfrac{t}{2})^5\right] + \ldots$$

$$+ \frac{a_n}{(2n+1)t^{2n}}\left[-(x - \tfrac{t}{2})^{2n+1} + (\tfrac{t}{2})^{2n+1}\right]. \qquad (11)$$

The bending moment at point x is

$$M_x = \int_o^x \int_o^x w\,dx^2 = \frac{a_o x^2}{2} + \frac{a_1}{12t^2}\left[(x - \tfrac{t}{2})^4 + 4(\tfrac{t}{2})^3 x - (\tfrac{t}{2})^4\right]$$

$$+ \frac{a_2}{30t^4}\left[(x - \tfrac{t}{2})^6 + 6(\tfrac{t}{2})^5 x - (\tfrac{t}{2})^6\right] + \ldots$$

$$+ \frac{a_n}{(2n+1)(2n+2)t^{2n}}\left[(x - \tfrac{t}{2})^{2n+2} + (2n+2)(\tfrac{t}{2})^{2n+1} x\right.$$

$$\left. - (\tfrac{t}{2})^{2n+2}\right], \qquad (12)$$

and at point $(t - x)$ the moment is

$$M_{(t-x)} = \int_o^{(t-x)} \int_o^x w\,dx^2 = \frac{a_o(t-x)^2}{2} + \frac{a_1}{12t^2}\left[(x - \tfrac{t}{2})^4\right.$$

$$\left. + 4(\tfrac{t}{2})^3 (t-x) - (\tfrac{t}{2})^4\right] + \frac{a_2}{30t^4}\left[(x - \tfrac{t}{2})^6 + 6(\tfrac{t}{2})^5 (t-x)\right.$$

$$- \left(\frac{t}{2}\right)^6\Big] + \ldots + \frac{a_n}{(2n+1)(2n+2)t^{2n}}\Big[\left(x - \frac{t}{2}\right)^{2n+2}$$

$$+ (2n+2)\left(\frac{t}{2}\right)^{2n+1}(t - x) - \left(\frac{t}{2}\right)^{2n+2}\Big]. \qquad (13)$$

A transformation of the reference axes to the thread midpoint can be made as indicated in Figure 4.

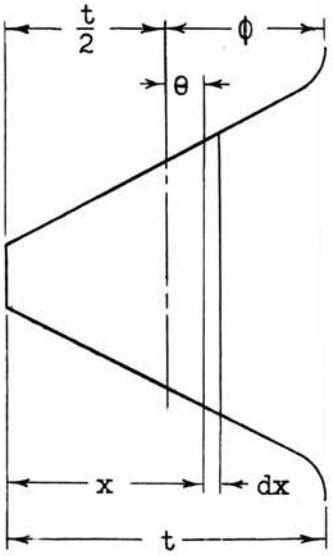

Fig. 4.—Transformation of the Reference Axes to Midpoint of the Thread

To accomplish this transformation, let

$$\theta = \left(x - \frac{t}{2}\right); \quad \phi = \left(\frac{t}{2}\right); \quad x = \theta + \phi;$$

then, the loading, shear, and moment equations become

$$w = a_o + a_1\left(\frac{\theta}{t}\right)^2 + a_2\left(\frac{\theta}{t}\right)^4 + \ldots + a_n\left(\frac{\theta}{t}\right)^{2n} = \sum_o^n a_n\left(\frac{\theta}{t}\right)^{2n}, \qquad (8a)$$

$$S_t = \int_o^t w\,dx = a_o(2\phi) + a_1\left(\frac{2\phi^3}{3t^2}\right) + a_2\left(\frac{2\phi^5}{5t^4}\right) + \ldots$$

$$+ \frac{a_n}{2n+1}\left(\frac{2\phi^{2n+1}}{t^{2n}}\right) = \sum_{o}^{n} \frac{a_n}{2n+1}\left(\frac{2\phi^{2n+1}}{t^{2n}}\right), \tag{9a}$$

$$S_x = \int_o^x w\,dx = a_o(\theta + \phi) + \frac{a_1}{3t^2}(\theta^3 + \phi^3) + \frac{a_2}{5t^4}(\theta^5 + \phi^5)$$

$$+ \ldots + \frac{a_n}{(2n+1)t^{2n}}(\theta^{2n+1} + \phi^{2n+1})$$

$$= \sum_{o}^{n} \frac{a_n(\theta^{2n+1} + \phi^{2n+1})}{(2n+1)t^{2n}}, \tag{10a}$$

$$S_{(t-x)} = \int_o^{(t-x)} w\,dx = a_o(\phi - \theta) + \frac{a_1}{3t^2}(\phi^3 - \theta^3) + \frac{a_2}{5t^4}(\phi^5 - \theta^5)$$

$$+ \ldots + \frac{a_n(\phi^{2n+1} - \theta^{2n+1})}{(2n+1)t^{2n}}$$

$$= \sum_{o}^{n} \frac{a_n(\phi^{2n+1} - \theta^{2n+1})}{(2n+1)t^{2n}}, \tag{11a}$$

$$M_x = \int_o^x \int_o^x w\,dx^2 = \frac{a_o}{2}(\theta + \phi)^2 + \frac{a_1}{12t^2}\left[\theta^4 + 4\phi^3(\theta + \phi) - \phi^4\right]$$

$$+ \frac{a_2}{30t^4}\left[\theta^6 + 6\phi^5(\theta + \phi) - \phi^6\right] + \ldots$$

$$+ \frac{a_n\left[\theta^{2n+2} + (2n+2)\phi^{2n+1}(\theta + \phi) - \phi^{2n+2}\right]}{(2n+1)(2n+2)t^{2n}}$$

$$= \sum_{o}^{n} \frac{a_n\left[\theta^{2n+2} + (2n+2)\theta\phi^{2n+1} + (2n+1)\phi^{2n+2}\right]}{(2n+1)(2n+2)t^{2n}}, \text{ and} \tag{12a}$$

$$M_{(t-x)} = \int_o^{(t-x)} \int_o^x w\,dx^2 = \frac{a_o(\phi - \theta)^2}{2} + \frac{a_1}{12t^2}\left[\theta^4 + 4\phi^3(\phi - \theta) - \phi^4\right]$$

$$+ \frac{a_2}{30t^4}\left[\theta^6 + 6\phi^5(\phi - \theta) - \phi^6\right] + \ldots$$

$$+ \frac{a_n\left[\theta^{2n+2} + (2n+2)\phi^{2n+1}(\phi - \theta) - \phi^{2n+2}\right]}{(2n+1)(2n+2)t^{2n}}$$

$$= \sum_{o}^{n} \frac{a_n\left[\theta^{2n+2} - (2n+2)\theta\phi^{2n+1} + (2n+1)\phi^{2n+2}\right]}{(2n+1)(2n+2)t^{2n}} . \quad (13a)$$

The loading curve is symmetric about the midpoint; that is,

$$\int_o^t w\,dx - \int_o^{(t-x)} w\,dx = \int_o^x w\,dx, \quad (14)$$

or

$$F - \int_o^{(t-x)} w\,dx = \int_o^x w\,dx, \quad (15)$$

and

$$F - \int_o^x w\,dx = \int_o^{(t-x)} w\,dx. \quad (16)$$

Substituting the above relations into Eqs. (7) and (3), the condition for an anti-symmetric curvature becomes

$$\left[\frac{\int_o^x\int_o^x w\,dx^2}{EC(J+\phi+\theta)^3} + \frac{\int_o^{(t-x)}\int_o^x w\,dx^2}{EC(J+\phi-\theta)^3} + \frac{k\int_o^x w\,dx}{GD(J+\phi+\theta)^2} + \frac{kF}{GD(J+\phi-\theta)^2}\right.$$

$$\left. - \frac{k\int_o^x w\,dx}{GD(J+\phi-\theta)^2} - \frac{kw}{GD(J+\phi+\theta)} - \frac{kw}{GD(J+\phi-\theta)}\right] = 0. \quad (17)$$

Let $J + \phi = H$; $EC = M$; $\frac{GD}{k} = N$. The common denominator becomes $MN(H+\theta)^3(H-\theta)^3$, so that Eq. (17) becomes

$$\left[N(H-\theta)^3\int_o^x\int_o^x w\,dx^2 + N(H+\theta)^3\int_o^{(t-x)}\int_o^x w\,dx^2 + 4MH\theta(\theta^2 - H^2)\int_o^x w\,dx\right.$$

$$\left. + M(H-\theta)(H+\theta)^3F - 2HM(H+\theta)^2(H-\theta)^2 w\right] = 0. \quad (18)$$

The first term of Eq. (18) is expanded by use of Eqs. (8a) through (13a) and becomes $N(H - \theta)^3 \int_o^x \int_o^x w\, dx^2 =$

$$\frac{a_o}{2} NH^3\phi^2 - \frac{3a_o}{2} NH^2\phi^2\theta + \frac{3a_o}{2} NH\phi^2\theta^2 - \frac{a_o}{2} N\phi^2\theta^3$$

$$+ a_o NH^3\phi\theta - 3a_o NH^2\phi\theta^2 + 3a_o NH\phi\theta^3 - a_o N\phi\theta^4$$

$$+ \frac{a_o}{2} NH^3\theta^2 - \frac{3a_o}{2} NH^2\theta^3 + \frac{3a_o}{2} NH\theta^4 - \frac{a_o}{2} N\theta^5$$

$$+ \frac{a_1 NH^3\phi^4}{4t^2} - \frac{3a_1 NH^2\phi^4\theta}{4t^2} + \frac{3a_1 NH\phi^4\theta^2}{4t^2} - \frac{a_1 N\phi^4\theta^3}{4t^2}$$

$$+ \frac{a_1 NH^3\phi^3\theta}{3t^2} - \frac{a_1 NH^2\phi^3\theta^2}{t^2} + \frac{a_1 NH\phi^3\theta^3}{t^2} - \frac{a_1 N\phi^3\theta^4}{3t^2}$$

$$+ \frac{a_1 NH^3\theta^4}{3\cdot 4t^2} - \frac{a_1 NH^2\theta^5}{4t^2} + \frac{a_1 NH\theta^6}{4t^2} - \frac{a_1 N\theta^7}{3\cdot 4t^2}$$

$$+ \frac{a_2 NH^3\phi^6}{6t^4} - \frac{a_2 NH^2\phi^6\theta}{2t^4} + \frac{a_2 NH\phi^6\theta^2}{2t^4} - \frac{a_2 N\phi^6\theta^3}{6t^4}$$

$$+ \frac{a_2 NH^3\phi^5\theta}{5t^4} - \frac{3a_2 NH^2\phi^5\theta^2}{5t^4} + \frac{3a_2 NH\phi^5\theta^3}{5t^4} - \frac{a_2 N\phi^5\theta^4}{5t^4}$$

$$+ \frac{a_2 NH^3\theta^6}{5\cdot 6t^4} - \frac{a_2 NH^2\theta^7}{10t^4} + \frac{a_2 NH\theta^8}{10t^4} - \frac{a_2 N\theta^9}{5\cdot 6t^4}$$

$$+ \ldots . \qquad (19)$$

The second term expanded becomes $N(H + \theta)^3 \int_o^{(t-x)} \int_o^x w\, dx^2 =$

$$\frac{a_o}{2} NH^3\phi^2 + \frac{3a_o}{2} NH^2\phi^2\theta + \frac{3a_o}{2} NH\phi^2\theta^2 + \frac{a_o}{2} N\phi^2\theta^3$$

$$- a_o NH^3\phi\theta - 3a_o NH^2\phi\theta^2 - 3a_o NH\phi\theta^3 - a_o N\phi\theta^4$$

$$+ \frac{a_o}{2} NH^3\theta^2 + \frac{3a_o}{2} NH^2\theta^3 + \frac{3a_o}{2} NH\theta^4 + \frac{a_o}{2} N\theta^5$$

$$+ \frac{a_1 NH^3\phi^4}{4t^2} + \frac{3a_1 NH^2\phi^4\theta}{4t^2} + \frac{3a_1 NH\phi^4\theta^2}{4t^2} + \frac{a_1 N\phi^4\theta^3}{4t^2}$$

$$- \frac{a_1 NH^3\phi^3\theta}{3t^2} - \frac{a_1 NH^2\phi^3\theta^2}{t^2} - \frac{a_1 NH\phi^3\theta^3}{t^2} - \frac{a_1 N\phi^3\theta^4}{3t^2}$$

$$+ \frac{a_1 NH^3\theta^4}{3\cdot 4t^2} + \frac{a_1 NH^2\theta^5}{4t^2} + \frac{a_1 NH\theta^6}{4t^2} + \frac{a_1 N\theta^7}{3\cdot 4t^2}$$

$$+ \frac{a_2 NH^3\phi^6}{6t^4} + \frac{a_2 NH^2\phi^6\theta}{2t^4} + \frac{a_2 NH\phi^6\theta^2}{2t^4} + \frac{a_2 N\phi^6\theta^3}{6t^4}$$

$$- \frac{a_2 NH^3\phi^5\theta}{5t^4} - \frac{3a_2 NH^2\phi^5\theta^2}{5t^4} - \frac{3a_2 NH\phi^5\theta^3}{5t^4} - \frac{a_2 N\phi^5\theta^4}{5t^4}$$

$$+ \frac{a_2 NH^3\theta^6}{5\cdot 6t^4} + \frac{a_2 NH^2\theta^7}{10t^4} + \frac{a_2 NH\theta^8}{10t^4} + \frac{a_2 N\theta^9}{5\cdot 6t^4}$$

$$+ \ldots . \qquad (20)$$

The third term expands to $4MH\theta(\theta^2 - H^2) \int_o^x w\, dx =$

$$- 4a_o MH^3\phi\theta - 4a_o MH^3\theta^2 + 4a_o MH\phi\theta^3 + 4a_o MH\theta^4$$

$$- \frac{4a_1 MH^3\phi^3\theta}{3t^2} - \frac{4a_1 MH^3\theta^4}{3t^2} + \frac{4a_1 MH\phi^3\theta^3}{3t^2} + \frac{4a_1 MH\theta^6}{3t^2}$$

$$- \frac{4a_2 MH^3\phi^5\theta}{5t^4} - \frac{4a_2 MH^3\theta^6}{5t^4} + \frac{4a_2 MH\phi^5\theta^3}{5t^4} + \frac{4a_2 MH\theta^8}{5t^4}$$

$$- \frac{4a_3MH^3\phi^7\theta}{7t^6} - \frac{4a_3MH^3\theta^8}{7t^6} + \frac{4a_3MH\phi^7\theta^3}{7t^6} + \frac{4a_3MH\theta^{10}}{7t^6}$$

$$- \ldots . \tag{21}$$

The fourth term, $M(H - \theta)(H + \theta)^3F$, becomes

$$FMH^4 + 2FMH^3\theta - 2FMH\theta^3 - FM\theta^4. \tag{22}$$

The fifth term is $- 2HM (H - \theta)^2 (H + \theta)^2 w =$

$$- 2a_oMH^5 + 4a_oMH^3\theta^2 - 2a_oMH\theta^4$$

$$- \frac{2a_1MH^5\theta^2}{t^2} + \frac{4a_1MH^3\theta^4}{t^2} - \frac{2a_1MH\theta^6}{t^2}$$

$$- \frac{2a_2MH^5\theta^4}{t^4} + \frac{4a_2MH^3\theta^6}{t^4} - \frac{2a_2MH\theta^8}{t^4}$$

$$- \frac{2a_3MH^5\theta^6}{t^6} + \frac{4a_3MH^3\theta^8}{t^6} - \frac{2a_3MH\theta^{10}}{t^6}$$

$$- \ldots . \tag{23}$$

The sum of coefficients of θ^o must vanish; that is,

$$\frac{a_oNH^3\phi^2}{2} + \frac{a_1NH^3\phi^4}{4t^2} + \frac{a_2NH^3\phi^6}{6t^4} + \frac{a_3NH^3\phi^8}{8t^6} + \frac{a_4NH^3\phi^{10}}{10t^8}$$

$$+ \ldots + \frac{a_nNH^3\phi^{2n+2}}{(2n + 2)t^{2n}} + \frac{FMH^4}{2} - a_oMH^5 = 0. \tag{24}$$

In the same manner, the coefficients of θ^1 are set equal to zero:

$$a_o MH^3\phi + \frac{a_1 MH^3\phi^3}{3t^2} + \frac{a_2 MH^3\phi^5}{5t^4} + \ldots + \frac{a_n MH^3\phi^{2n+1}}{(2n+1)t^{2n}} - \frac{FMH^3}{2} = 0. \quad (25)$$

The equation for coefficients of $\theta^2 = 0$ becomes

$$\frac{3a_o NH\phi^2}{2} - 3a_o NH^2\phi + \frac{a_o NH^3}{2} + \frac{3a_1 NH\phi^4}{4t^2} - \frac{3a_1 NH^2\phi^3}{3t^2} + \frac{3a_2 NH\phi^6}{6t^4}$$

$$- \frac{3a_2 NH^2\phi^5}{5t^4} + \ldots + \frac{3a_n NH\phi^{2n+2}}{(2n+2)t^{2n}} - \frac{3a_n NH^2\phi^{2n+1}}{(2n+1)t^{2n}} - \frac{a_1 MH^5}{t^2}$$

$$= 0. \quad (26)$$

The equation for coefficients of $\phi^3 = 0$ is

$$a_o MH\phi + \frac{a_1 MH\phi^3}{3t^2} + \frac{a_2 MH\phi^5}{5t^4} + \frac{a_3 MH\phi^7}{7t^6} + \ldots + \frac{a_n MH\phi^{2n+1}}{(2n+1)t^{2n}}$$

$$- \frac{FMH}{2} = 0, \quad (25a)$$

which is the same as Eq. (25).

The coefficients of θ^4 are related by

$$- a_o N\phi + \frac{3a_o NH}{2} - \frac{a_1 N\phi^3}{3t^2} + \frac{a_1 NH^3}{3\cdot 4t^2} - \frac{a_2 N\phi^5}{5t^4} - \frac{a_3 N\phi^7}{7t^6}$$

$$- \ldots - \frac{a_n N\phi^{2n+1}}{(2n+1)t^{2n}} + a_o MH - \frac{F}{2} + \frac{4a_1 MH^3}{3t^2} - \frac{a_2 MH^5}{t^4}$$

$$= 0. \quad (27)$$

There are no terms containing θ^5; in fact, there are no odd powers of θ greater than θ^3.

Finally, the coefficients of θ^6 yield

$$\frac{a_1 NH}{4t^2} + \frac{a_2 NH^3}{5\cdot 6t^4} - \frac{a_1 MH}{3t^2} + \frac{8a_2 MH^3}{5t^4} - \frac{a_3 MH^5}{t^6} = 0. \tag{28}$$

Equations (25) and (25a) are identical; thus, only five equations have been obtained. It is possible, however, to obtain the series expression for w through a_4 with the equations at hand. These equations after rearrangement become

$$a_0\left(\frac{\phi^2}{2} - \frac{MH^2}{N}\right) + a_1\left(\frac{\phi^4}{4t^2}\right) + a_2\left(\frac{\phi^6}{6t^4}\right) + a_3\left(\frac{\phi^8}{8t^6}\right) + a_4\left(\frac{\phi^{10}}{10t^8}\right) = -\frac{FMH}{2N}, \tag{29}$$

$$a_0\phi + \frac{a_1\phi^3}{3t^2} + \frac{a_2\phi^5}{5t^4} + \frac{a_3\phi^7}{7t^6} + \frac{a_4\phi^9}{9t^8} = \frac{F}{2}, \tag{30}$$

$$a_0\left(\frac{3}{2}\phi^2 - 3H\phi + \frac{H^2}{2}\right) + a_1\left(\frac{3\phi^4}{4t^2} - \frac{H\phi^3}{t^2} - \frac{MH^4}{Nt^2}\right) + a_2\left(\frac{\phi^6}{2t^4} - \frac{3H\phi^5}{5t^4}\right)$$

$$+ a_3\left(\frac{3\phi^8}{8t^6} - \frac{3H\phi^7}{7t^6}\right) + a_4\left(\frac{3\phi^{10}}{10t^8} - \frac{H\phi^9}{3t^8}\right) = 0, \tag{31}$$

$$a_0\left(-N\phi + \frac{3NH}{2} + MH\right) + a_1\left(-\frac{N\phi^3}{3t^2} + \frac{NH^3}{3\cdot 4t^2} + \frac{4MH^3}{3t^2}\right) - a_2\left(\frac{N\phi^5}{5t^4} + \frac{MH^5}{t^4}\right)$$

$$- a_3\left(\frac{N\phi^7}{7t^6}\right) - a_4\left(\frac{N\phi^9}{9t^8}\right) = \frac{FM}{2}, \text{ and} \tag{32}$$

$$a_1\left(\frac{N}{4} - \frac{M}{3}\right) + a_2\left(\frac{NH^2}{30t^2} + \frac{8MH^2}{5t^2}\right) - a_3\left(\frac{MH^4}{t^4}\right) = 0. \tag{33}$$

The five equations containing five unknown coefficients may now be

solved simultaneously for a given size thread having known physical properties, provided that stresses are below the elastic limit of the material. As an example, the one-inch modified Whitworth thread given by Mrs. Fila[5] will be used, giving

$$t = 0.08 \text{ inch},$$

$$\phi = \left(\frac{t}{2}\right) = 0.04 \text{ inch},$$

$$J = \left(\frac{ct}{p-c}\right) = 0.02 \text{ inch},$$

$$H = (J+\phi) = 0.06 \text{ inch},$$

$$c = \frac{B}{12}\left(\frac{p-c}{t}\right)^3 = 0.094B, \text{ and}$$

$$D = B\left(\frac{p-c}{t}\right) = 1.04B.$$

For Bakelite, Hetényi[6] gives

$$E = 1100 \text{ psi}, \quad \mu = 0.5, \text{ and}$$

$$G = \frac{E}{2(1-\mu)} = \frac{1100}{2(1-0.5)} = 367 \text{ psi}.$$

Thus, the constants M and N become

$$M = EC = 103.4B, \text{ lb./in., and}$$

$$N = GD/k = 254.22B, \text{ lb./in.}$$

Substituting these values into Eqs. (27) through (31) and solving simultaneously will lead to the following values of the

---

[5]Fila, op. cit., p. 25.

[6]M. Hetényi, Handbook of Experimental Stress Analysis (New York, 1950), p. 894.

coefficients:

$$a_o = + 14.764F,$$

$$a_1 = - 42.842F,$$

$$a_2 = + 10.426F,$$

$$a_3 = - 6.916F, \text{ and}$$

$$a_4 = + 2779.259F.$$

Equation (8a), giving the radial load distribution across the thread may now be evaluated. Table 1 gives the load obtained at increments of 0.01 inch across the tooth.

Table 1. Calculated Values of Load Distribution, w/F

x	0.0	0.01	0.02	0.03	0.04
θ	- 0.04	- 0.03	- 0.02	- 0.01	0.0
θ/t	- 0.5	- 0.375	- 0.25	- 0.125	0.0
a_o	+ 14.764F	+ 14.764F	+ 14.764F	+ 14.764F	+ 14.764F
$a_1(\frac{\theta}{t})^2$	- 10.710F	- 6.024F	- 2.677F	- 0.669F	0.0
$a_2(\frac{\theta}{t})^4$	+ 0.652F	+ 0.206F	+ 0.041F	+ 0.003F	0.0
$a_3(\frac{\theta}{t})^6$	- 0.108F	- 0.019F	- 0.002F	0.0	0.0
$a_4(\frac{\theta}{t})^8$	+ 10.856F	+ 1.087F	+ 0.042F	0.0	0.0
w/F	+ 15.454	+ 10.014	+ 12.168	+ 14.097	+ 14.764

Figure 5, page 21, is a plot of the load distribution versus the

radial distance x.

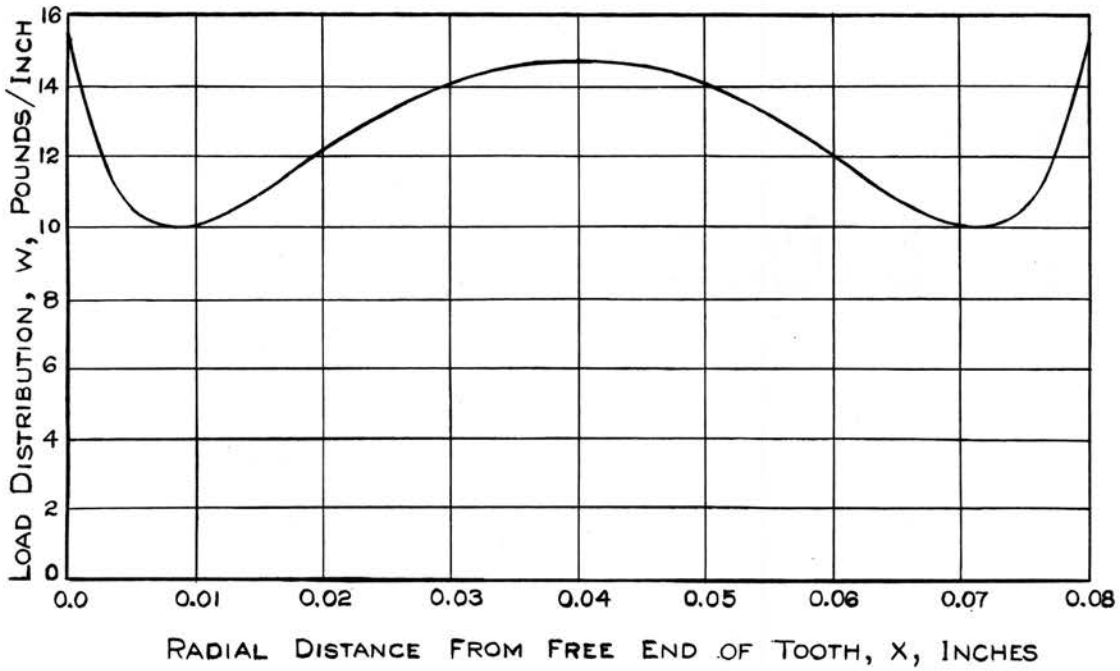

Fig. 5.—Radial Load Distribution Curve

Attention is called to the fact that the load distribution has been obtained in terms of the constant (1/F). Since this constant does not affect subsequent results, it is arbitrarily omitted in all further tables and equations.

A Check on the Loading Curve

One of the necessary conditions which the loading curve must satisfy has been achieved during its derivation; namely, the curvature must be anti-symmetric with respect to the midpoint of the tooth segment. There remains the task of checking the requirements imposed by Eqs. (1) and (2). One way in which this may be accomplished is to integrate the loading curve successively until the slope and deflection curves have been obtained. If the slope curve is then symmetric and

the deflection curve anti-symmetric with respect to the midpoint of the tooth, Eqs. (1) and (2) will have been satisfied.

Niles and Newell have shown a system of tabular integration which will be adapted to the case at hand in order to yield values of the shear and moment due to load.[7] The calculated results are shown in Table 2, page 23.

The slope and deflection curves may now be obtained by integrating the curvature equation, M_x/EI_x, if one remembers that both the area and moment of inertia of the section vary with x. Equation (7) shows the portions of the elastic and shear loads which, when integrated, will result in deflections of the tooth due to flexure and shear, respectively.

The first term on the right side of Eq. (7) gives the elastic load which produces deflection due to flexure,

$$\frac{\int_o^x \int_o^x w\, dx^2}{EI_x} = \left(\frac{d^2y}{dx^2}\right)_f. \tag{34}$$

Then, the slope and deflection are

$$\left(\frac{dy}{dx}\right)_f = \int_o^x \frac{\int_o^x \int_o^x w\, dx^3}{EI_x} + C_1, \tag{35}$$

$$y_f = \int_o^x \left(\frac{dy}{dx}\right)_f dx + C_2, \tag{36}$$

and since $\left(\frac{dy}{dx}\right)_f = y_f = 0$ at $x = t$, then the constants are

---

[7]Alfred S. Niles and Joseph S. Newell, Airplane Structures (New York, 1943), I, p. 56.

Table 2. Calculated Values of Shear, S_x, and Moment, M_x

(1)	x	0	0.01	0.02	0.03	0.04	0.05	0.06	0.07	0.08
(2)	w	15.454	10.014	12.168	14.098	14.764	14.098	12.168	10.014	15.454
(3)	Mean w Ordinate		11.64	11.09	13.13	14.43	14.43	13.13	11.09	11.64
(4)	$S_x = \int_o^x w\,dx$	0	0.1164	0.2273	0.3586	0.5029	0.6472	0.7785	0.8894	1.0058
(5)	Mean S_x Ordinate		0.0582	0.1719	0.2930	0.4308	0.5750	0.7128	0.8340	0.9476
(6)	$M_x = \int_o^x \int_o^x w\,dx$	0	0.000582	0.00230	0.00523	0.00954	0.01529	0.02242	0.03075	0.040225

$$C_1 = - \int_o^t \frac{\int_o^x \int_o^x w \, dx^3}{EI_x} ; \tag{37}$$

$$C_2 = - \int_o^t (\frac{dy}{dx})_f \, dx. \tag{38}$$

The results of the integration of the elastic load are tabulated in Table 3, page 25.

Curvature due to shear is represented by the last two terms on the right hand side of Eq. (7) as

$$(\frac{d^2y}{dx^2})_s = - \frac{kw}{AG} + \frac{k \int_o^x w \, dx}{A^2 G} (\frac{dA}{dx}). \tag{39}$$

The slope and deflection due to shear are

$$(\frac{dy}{dx})_s = - \frac{k \int_o^x w \, dx}{A_x G} + C_3 \tag{40}$$

and

$$y_s = - k \int_o^x (\frac{dy}{dx})_s \, dx + C_4, \tag{41}$$

and the constants may be evaluated, since

$$\text{at } x = 0, \quad (dy/dx)_s = 0, \text{ and } C_3 = 0,$$

while

$$\text{at } x = t, \quad y_s = 0, \text{ and } C_4 = k \int_o^t (\frac{dy}{dx})_s \, dx.$$

The results of the integration of the shear load are tabulated in Table 4, page 26, and show the slope and deflection due to shear.

Table 3. Calculated Values of Slope, $(dy/dx)_f$, and Deflection, y_f, Due to Flexure

(1)	x	0	0.01	0.02	0.03	0.04	0.05	0.06	0.07	0.08
(7)	$\frac{\int_o^x \int_o^x w\, dx^2}{EI_x}$	0	0.208	0.348	0.405	0.4275	0.431	0.424	0.408	0.389
(8)	Mean Ordinate of (7)		0.104	0.278	0.377	0.416	0.429	0.428	0.416	0.399
(9)	$\int_o \frac{\int_o^x \int_o^x \int_o^x w\, dx^3}{EI_x}$	0	0.00104	0.00382	0.00759	0.01175	0.01604	0.02032	0.02448	0.02847 $= -C_1$
(10)	$(dy/dx)_f$	-0.02847	-0.02743	-0.02465	-0.02088	-0.01672	-0.01243	-0.00815	-0.00400	0
(11)	Mean Ordinate of (10)		-0.02795	-0.02604	-0.02277	-0.01880	-0.01458	-0.01029	-0.00608	-0.002
(12)	$\int_o^x (\frac{dy}{dx})_f\, dx$	0	-0.000280	-0.000540	-0.000768	-0.000956	-0.001101	-0.001204	-0.001265	-0.001285 $= -C_2$
(13)	y_f	0.001285	0.001005	0.000745	0.000517	0.000329	0.000184	0.000081	0.00002	0

Table 4. Calculated Values of Slope, $(dy/dx)_s$, and Deflection, y_s, Due to Shear

(1)	x	0	0.01	0.02	0.03	0.04	0.05	0.06	0.07	0.08
(14)	$(\frac{dy}{dx})_s = -\frac{k\int_o^x w\,dx}{EI_x}$	0	-0.0150	-0.0224	-0.0282	-0.0330	-0.0364	-0.0382	-0.0388	-0.0396
(15)	Mean Ordinate of (14)	-0.0075	-0.0187	-0.0253	-0.0306	-0.0346	-0.0373	-0.0385	-0.0392	
(16)	$-k\int_o \frac{\int_o^x \int_o^x w\,dx^2}{A_x G}$	0	-0.000075	0.000262	0.000515	0.000821	0.001167	0.001540	0.001925	-0.002320 $= -C_4$
(17)	y_s	0.00232	0.00224	0.00206	0.00181	0.00150	0.00115	0.00078	0.00039	0

Total slope and deflection for the tooth are the sums of their components due to flexure and shear. When the values for these components are taken from Tables 3 and 4, pages 25 and 26, respectively, the total slope and deflection will be as indicated in Table 5, page 28. These calculated values are shown graphically in Figs. 6 and 7, page 29, and clearly indicate the relationship of each of the curves to the midpoint of the tooth. The total slope curve is very nearly symmetric with respect to the midpoint of the tooth, and the total deflection is anti-symmetric; therefore, the necessary conditions of Eqs. (1) and (2) regarding these curves have been met, and the loading distribution, w, has fulfilled all the conditions required by an anti-symmetric deflection curve.

Table 5. Calculated Values of Total Slope, dy/dx, and Deflection, y

(1) x	0	0.01	0.02	0.03	0.04	0.05	0.06	0.07	0.08
(10) $(dy/dx)_f$	-0.02847	-0.02743	-0.02465	-0.02088	-0.01672	-0.01243	-0.00815	-0.00400	0
(14) $(dy/dx)_s$	0	-0.0150	-0.0224	-0.0282	-0.0330	-0.03640	-0.03820	-0.0388	-0.0396
(18) dy/dx = (10) + (14)	-0.02847	-0.04243	-0.04705	-0.04908	-0.04972	-0.04883	-0.04635	-0.0428	-0.0396
(13) y_f	0.001285	0.001005	0.000745	0.000517	0.000329	0.000184	0.000081	0.000020	0
(17) y_s	0.00232	0.00224	0.00206	0.00181	0.00150	0.00115	0.00078	0.00039	0
(19) y = (13)+(17)	0.003605	0.003245	0.002805	0.002327	0.001829	0.001334	0.000861	0.00041	0

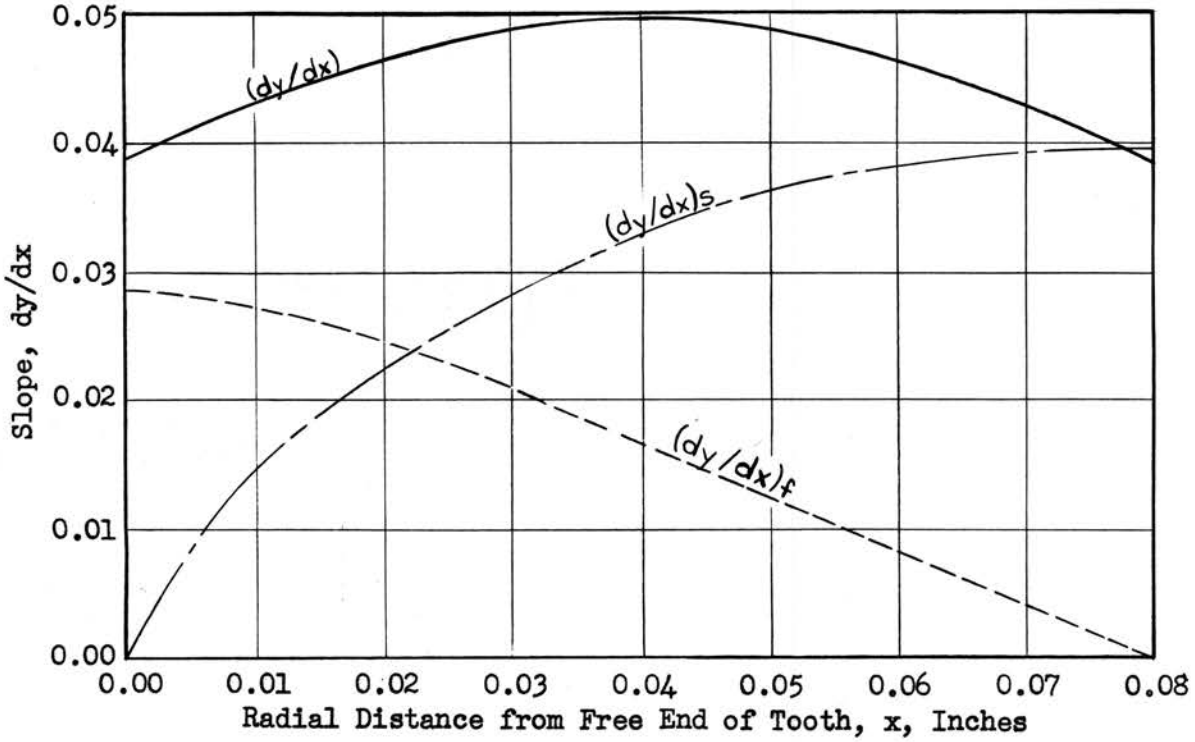

Fig. 6.—Slope due to flexure and shear shown to be symmetric with respect to midpoint of the tooth.

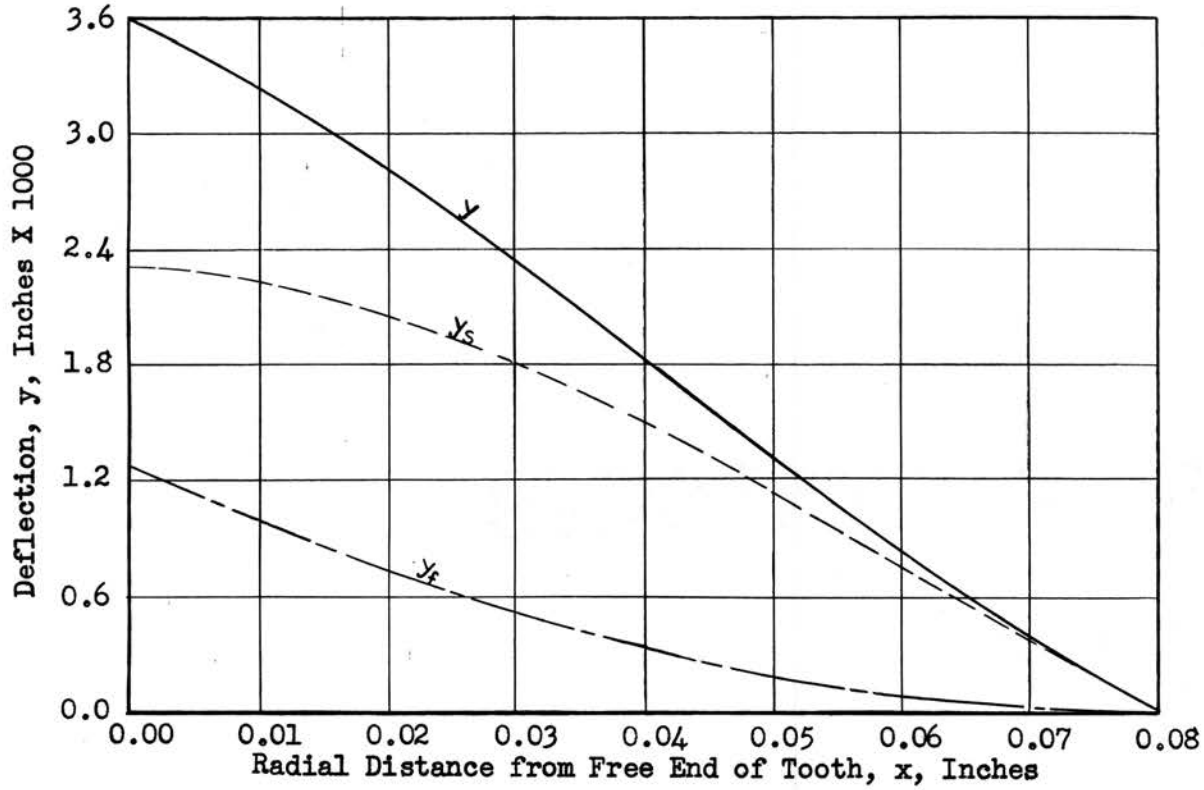

Fig. 7.—Deflection due to flexure and shear shown to be anti-symmetric with respect to midpoint of the tooth.

CHAPTER III

THE RIGIDITY CONSTANT

Derivation

The hypothetical elastic layer may be used in design of screw threads if a suitable theory can show that the layer has the same properties as the screw thread it replaces. Using the method of least work, Gertrude H. Fila has shown that good agreement may be had between the theoretical axial stress distribution and experimental results if the theoretical elastic layer has the same rigidity as the actual thread.[1] The remaining task is to show that the radial load distribution with its resulting thread deflection will yield a rigidity constant which will be an improvement over that obtained by Mrs. Fila.

The rigidity of the tooth may be evaluated by considering the work done by the load while deflecting the tooth. For an elastic layer, the shear stress is shown by Raymond E. Chapel to be proportional to the deflection;[2] or,

$$s_s = Ky_{max}. \tag{42}$$

The elemental section of elastic layer is shown in Figure 8, page 31, for a shear load applied in the axial direction.

---

[1]Gertrude H. Fila, "Load Distribution in Screw Threads by the Method of Least Work" (unpublished M. S. thesis, Department of Mechanical Engineering, Oklahoma A. & M. College, 1952), p. 24.

[2]Raymond E. Chapel, "A Contribution to the Theory of Load Distribution in Screw Threads" (unpublished M. S. thesis, Department of Mechanical Engineering, Oklahoma A. & M. College, 1951), p. 8.

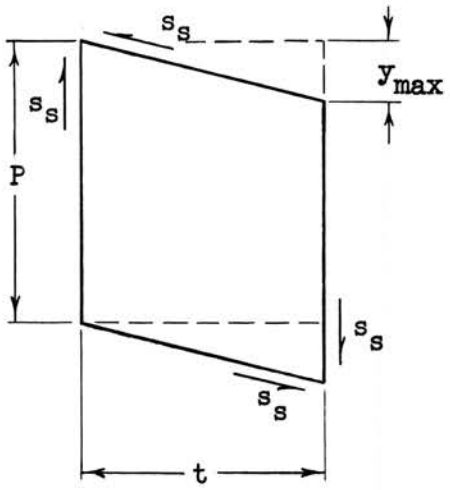

Fig. 8.—Elemental Section of Elastic Layer Under Load

The work done on the elastic layer is

$$W = \frac{1}{2} s_s A y_{max}, \tag{43}$$

where, if A, the tooth cross-sectional area, is taken as the unit width of the tooth segment multiplied by the screw thread pitch P, the substitution of Eq. (42) into Eq. (43) will give for the work

$$W = \frac{1}{2} K P y_{max}^2. \tag{44}$$

At any point x on the actual tooth, the work done by the local load $w \Delta x$ moving through the deflection distance y will be

$$\Delta W = 2wy \Delta x, \tag{45}$$

since two mating threads are involved within the area defined by P. The total work accomplished by the radial load distributed over the tooth segments is, therefore,

$$W = 2 \sum_{o}^{t} wy \, \Delta x. \tag{46}$$

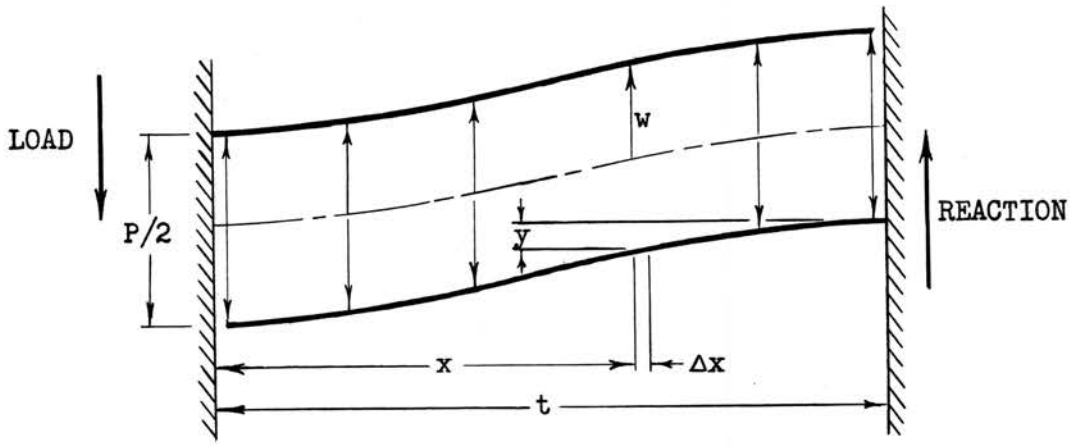

Fig. 9.—Tooth Segment Under Theoretical Radial Load Distribution

Since the work done by a load on the elastic layer must be identical to that done on the actual tooth, Eqs. (44) and (46) may be equated to obtain the rigidity constant

$$K = \frac{4 \sum_{o}^{t} wy\Delta x}{Py^2_{max}} . \tag{47}$$

Application

In order to evaluate Eq. (47), values for load distribution, w, and deflection, y, will be taken from Tables 2 and 5, pages 23 and 28, respectively. The term $\sum_{o}^{t} wy \, \Delta x$ may then be obtained by tabular integration, the results being as tabulated in Table 6, page 33. For a screw pitch, P, of 0.125 inch, and maximum deflection of 0.003605 inch,

Table 6. Work Done by the Theoretical Radial Load During Tooth Deflection

(1)	x	0.0	0.01	0.02	0.03	0.04	0.05	0.06	0.07	0.08
(2)	w	15.454	10.014	12.168	14.098	14.764	14.098	12.168	10.014	15.454
(3)	Mean w Δx		0.1164	0.1109	0.1313	0.1443	0.1443	0.1313	0.1109	0.1164
(4)	y	0.003605	0.003245	0.002805	0.002327	0.001829	0.001334	0.000861	0.000410	0.0
(5)	Mean y		0.003425	0.003025	0.002566	0.002078	0.001582	0.001098	0.000636	0.000205
(6)	wy Δx = (3)x(5)		0.000399	0.000335	0.000337	0.0003	0.000229	0.000144	0.000071	0.000024
(7)	$\sum_{o}^{x}$ wy Δx	0.0	0.000399	0.000734	0.001071	0.001371	0.001600	0.001744	0.001815	0.001839

the rigidity constant becomes

$$K = \frac{4 \sum_{o}^{t} wy \, \Delta x}{Py_{max}^{2}} = \frac{4(0.001839)}{0.125(1.3 \times 10^{-5})} = 4525, \qquad (48)$$

or, in terms of the modulus of elasticity,[3] E = 1100 psi,

$$K = \frac{4525 \, E}{1100} = 4.114 \, E. \qquad (49)$$

The value of K thus determined may be compared with that obtained by Mrs. Fila,[4] which is

$$K = 1.542 \, E.$$

Since the rigidity constant given by the radial load distribution is greater than that obtained by Mrs. Fila by assuming the load to be concentrated at the free end of the tooth, it is seen that the distributed load will, in effect, produce an elastic layer which is more rigid, and will, therefore, result in higher stress concentration than the layer evolved by Mrs. Fila. This is undesirable, since Mrs. Fila's theoretical stress concentration curve was already slightly higher than Mr. Hetényi's experimental stress curve. It must be concluded that the theoretical radial load which was intended to be an improvement over Mrs. Fila's work has, in truth, been a step in the wrong direction.

In order to determine the change involved when the rigidity constant is obtained by use of the distributed load, the axial stress

---

[3] M. Hetényi, Handbook of Experimental Stress Analysis (New York, 1950), p. 894.

[4] Fila, op. cit., p. 27.

concentration will now be calculated by means of Mrs. Fila's equation giving the ratio of the stress at any axial point x to the mean stress in the thread,[5]

$$\frac{s_x}{s_m} = \frac{n\ell}{\sinh(n\ell)} \left[\cosh(n\ell - nx)\right], \tag{50}$$

where $n = \left[\frac{\pi DK}{E}\left(\frac{1}{A_1} + \frac{1}{A_2}\right)\right]^{\frac{1}{2}} = 5.8,$

A_1 = bolt area in tension = 0.554 square inch,

A_2 = nut area in compression = 0.982 square inch,

D = mean diameter of elastic layer = 0.92 inch,

K = 4.114 E, and

ℓ = length of threaded joint = 1 inch.

Values of s_x/s_m have been calculated for intervals of one tenth of an inch along the axial length of the threaded joint as indicated in Table 7.

Table 7. Calculated Values of Stress Concentration, s_x/s_m

x	$\frac{n\ell}{\sinh(n\ell)}$	nx	$(n\ell - nx)$	cosh $(n\ell - nx)$	s_x/s_m
0.0	0.0351	0.0	5.80	165.15	5.8
0.1		0.58	5.22	92.55	3.25
0.2		1.16	4.64	51.84	1.82
0.3		1.74	4.06	29.03	1.03
0.4		2.32	3.48	16.249	0.57
0.5		2.90	2.90	9.115	0.32
0.6		3.48	2.32	5.137	0.18
0.7		4.06	1.74	2.936	0.103
0.8		4.64	1.16	1.752	0.0615
0.9		5.22	0.58	1.173	0.0412
1.0	0.0351	5.80	0.00	1.000	0.0351

[5]Ibid., p. 17.

The resultant stress-concentration curve is shown in Fig. 10, in comparison with the modified experimental stress curve of Mr. Hetényi and the theoretical stress curve obtained by Mrs. Fila.[6]

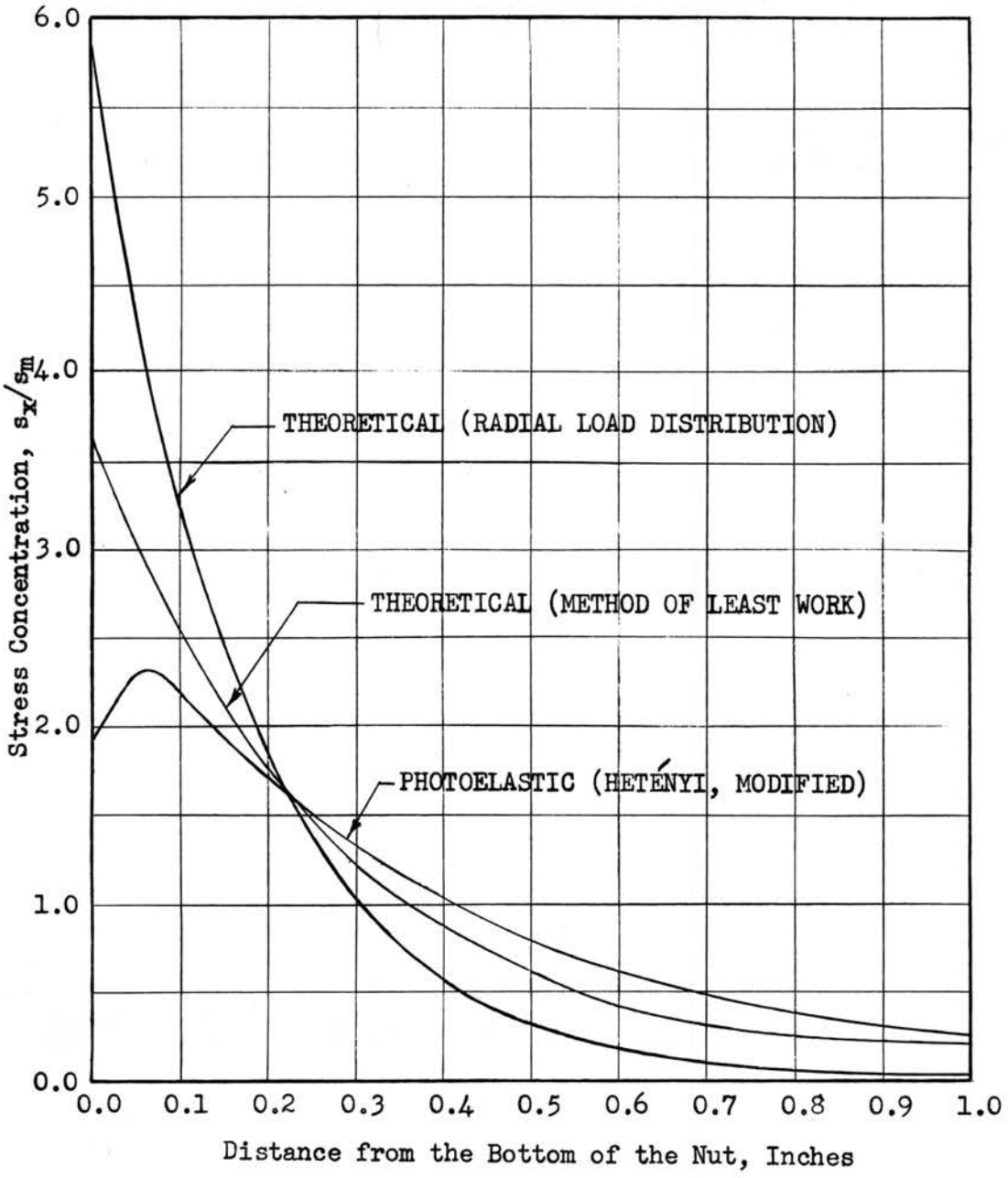

Fig. 10.—Stress Concentration Curves, s_x/s_m

---

[6] Ibid., p. 18.

CHAPTER IV

SUMMARY AND CONCLUSIONS

The object of this investigation was to determine a theoretical radial load distribution in screw threads by considering the effects of both bending and shear upon the thread tooth. Once the load distribution was obtained, it was hoped that the theory could be used to yield a rigidity constant for a hypothetical elastic layer which would be an improvement over the one which Gertrude H. Fila derived by considering only deflection due to bending.[1] The extent to which the theory failed in the latter objective was shown graphically in Fig. 10, page 36, which depicts the two theoretical stress-concentration curves superimposed upon the experimental curve M. Hetényi secured by means of an annealed Bakelite photoelastic model.[2] As may be seen, the theoretical stress-concentration curve obtained by Mrs. Fila is a much better approximation to the experimental curve than was obtained by means of the theoretical radial load distribution.

The most probable reason that the present work produces a more rigid thread with higher stress concentration is that the derivation of the loading curve demanded that the curvature due to bending and shear be anti-symmetric with respect to the midpoint of the tooth segment. Obviously, this condition does not exist in the region near the last

---

[1]Gertrude H. Fila, "Load Distribution in Screw Threads by the Method of Least Work" (unpublished M. S. thesis, Department of Mechanical Engineering, Oklahoma A. & M. College, 1952), p. 24.

[2]Ibid., p. 18.

engaged thread, since the free end of the thread is not rigidly restrained by the roots of the mating threads as has been assumed in this work.

By granting the fact that none of the assumptions made during the derivation of the radial load distribution are quite precise, some information gleaned from the theory stands out:

1. The maximum deflection of the tooth segment due to shear is approximately twice the maximum deflection due to bending (see Fig. 7, page 29).
2. Although the magnitude of the load distribution is greatest at the ends of the tooth segment, for all practical purposes, the load distribution may be considered constant (see Fig. 5, page 21).

With a constant load distribution, the deflection curve may be obtained easily by formal integration. Any further development of the elastic-layer theory can make use of this fact to improve upon the value of the rigidity constant.

BIBLIOGRAPHY

Chapel, Raymond E. "A Contribution to the Theory of Load Distribution in Screw Threads." Unpublished Master's Thesis, Department of Mechanical Engineering, Oklahoma A. & M. College, 1951.

Fila, Gertrude H. "Load Distribution in Screw Threads by the Method of Least Work." Unpublished Master's Thesis, Department of Mechanical Engineering, Oklahoma A. & M. College, 1952.

Hetényi, Milkós Imre. Handbook of Experimental Stress Analysis. New York: John Wiley and Sons, Inc., 1950.

------. "A Photoelastic Study of Bolt and Nut Fastenings." American Society of Mechanical Engineers Transactions, 65 (1943), A-93 through A-100.

Niles, Alfred S., and Joseph S. Newell. Airplane Structures. New York: John Wiley and Sons, Inc., Vol. I, 1943.

Oberg, Erik, and F. D. Jones. Machinery's Handbook. New York: The Industrial Press, 1941.

Timoshenko, S., and G. H. MacCullough. Elements of Strength of Materials. New York: D. Van Nostrand Company, Inc., 1935.

VITA

RICHARD MILLARD GILMORE
candidate for the degree of
Master of Science

Thesis: A THEORETICAL RADIAL LOAD DISTRIBUTION IN SCREW THREADS

Major: Mechanical Engineering

Minor: None

Biographical and Other Items:

Born: November 6, 1921, at Chicago, Illinois.
Undergraduate Study: Oklahoma Agricultural and Mechanical College, 1940-1942 (Certificate in Technical Machine Shop); Oklahoma Agricultural and Mechanical College, 1949-1952.
Graduate Study: Oklahoma Agricultural and Mechanical College, 1952-1953.
Experience: Aviation Machinist's Mate, U. S. Navy, 1942-1945; Naval Flight Student, 1945-1947; Naval Aviator, 1947-1949; Student Instructor, Spring, 1952; Research Assistant, 1952-1953; Instructor in Mechanical Engineering, 1953.

Date of Final Examination: May, 1953.

THESIS TITLE: A THEORETICAL RADIAL LOAD DISTRIBUTION IN SCREW THREADS

AUTHOR: Richard Millard Gilmore

THESIS ADVISER: Professor Ladislaus J. Fila

The content and form have been checked and approved by the author and thesis adviser. The Graduate School Office assumes no responsibility for errors either in form or content. The copies are sent to the bindery just as they are approved by the author and faculty adviser.

TYPIST: Albiette G. Gilmore